

## Ion distribution in multilayers of weak polyelectrolytes: A neutron reflectometry study

Oleh M. Tanchak,<sup>1</sup> Kevin G. Yager,<sup>1</sup> Helmut Fritzsche,<sup>2</sup> Thad Harroun,<sup>2,3</sup> John Katsaras,<sup>2,4</sup> and Christopher J. Barrett<sup>1,a)</sup>

<sup>1</sup>*Department of Chemistry, McGill University, Montreal H3A 2K6, Canada*

<sup>2</sup>*Canadian Neutron Beam Centre, National Research Council Canada, Chalk River K0J 1J0, Canada*

<sup>3</sup>*Department of Physics, University of Guelph, Guelph N1G 2W1, Canada*

<sup>4</sup>*Guelph-Waterloo Physics Institute and the Biophysics Interdepartmental Group, University of Guelph, Guelph N2L 3G1, Ontario, Canada*

(Received 18 February 2008; accepted 19 May 2008; published online 22 August 2008)

Neutron reflectometry was used to determine the distribution of salt ions and water in thin poly(acrylic acid) and poly(allylamine hydrochloride) polyelectrolyte multilayers assembled with and without salt. Increasing salt concentration reverses the exclusion of water from the substrate region, eventually leading to an asymmetric segregation of water near the substrate at high salt concentration. The counterions were found to localize near the substrate in films that were either assembled with salt or were exposed to salt solutions. In addition, the capping layer of the film was found to greatly influence the counterion distribution in the multilayer. © 2008 American Institute of Physics. [DOI: 10.1063/1.2943201]

### INTRODUCTION

The electrostatic interaction between two oppositely charged polyelectrolyte chains is the main driving force for the formation of polyelectrolyte multilayers (PEMs). The alternating adsorption of two oppositely charged polyelectrolytes onto a substrate using the layer-by-layer (LbL) technique can produce thin multilayer films with well-defined composition, thickness, and surface properties.<sup>1</sup> With weak polyelectrolyte systems, the degree of ionization of both polymer systems (polyacid and polybase) can be regulated by varying the solution pH, which allows for further control of film properties.<sup>2</sup> The ability of the LbL method to form thin films that are structurally diverse has attracted intense interest for building novel systems with many potential applications including sensors,<sup>3,4</sup> optical devices,<sup>4,5</sup> separation membranes,<sup>6</sup> and drug delivery vehicles.<sup>7</sup>

PEM systems can respond to environmental factors, such as water exposure, pH, and salt concentration. The ability to predict the behavior and response of these systems, in particular, on the microscale, is of fundamental importance. Knowledge of the internal properties of the PEMs may give insight to further fine-tune film properties in order to produce novel materials. The interaction of water with polyelectrolyte thin films is crucial, yet still not fully understood. Recently it has been found that the water distribution within weak polyelectrolyte thin films is asymmetric, with water localizing preferentially at the polymer surface, whether or not the films are swollen from a humid atmosphere or using bulk water.<sup>8</sup> The determination of the water profile in these PEMs helped to explain the anomalous swelling kinetics previously observed in these systems.<sup>9</sup> However, the effect of pH and

counterions on the water distribution in PEMs has not been fully elucidated, and reported experimental results are contradictory with regard to the role of salt and counterions in the formation of these PEMs.<sup>10</sup>

Recently neutron reflectometry studies on poly[5-(2-trifluoromethyl-1,1,1-trifluoro-2-hydroxypropyl)-2-norbornene] spin cast polyelectrolyte films have indicated a depletion of the counterion near the substrate of the film and an enrichment near the film's free surface.<sup>11</sup> Although these experiments revealed the distribution of base counterions within the film, the study was not performed with a multilayer system. In this paper, we provide a direct measurement of the water association and counterion distribution inside weak poly(acrylic acid) and poly(allylamine hydrochloride) (PAA/PAH) PEMs, when treated postassembly with varying solution pH and salt conditions. Using specular neutron reflectometry, the water and counterion distributions in PAA/PAH assembled films were measured, both *in situ* during exposure to a salt solution and on dried films after salt exposure. In order to mask the contribution of the water we made use of the so-called null-scattering water, which consists of a 8:92 mixture of H<sub>2</sub>O and D<sub>2</sub>O with scattering lengths of -1.675 and +19.145 fm, respectively. This mixture has a zero scattering length density (SLD) and is therefore invisible in a neutron reflectometry experiment. These experiments provide a clear picture of the distribution of salt ions in PEMs and demonstrate that the water distribution is strongly affected by salt localization. These insights are critical for the development of further applications.

### EXPERIMENTAL

#### Materials and film assembly

PAH ( $M_w=60\,000$  g/mol) was purchased from Aldrich, while PAA ( $M_w=90\,000$  g/mol) was obtained from Poly-

<sup>a)</sup>Author to whom correspondence should be addressed. Electronic addresses: christopher.barrett@mcgill.ca and chris.barrett@mcgill.ca.

sciences as a 25% aqueous solution. The polyelectrolytes were used as received without further purification. Polyelectrolyte solutions of  $10^{-2}M$  (concentration based on monomer unit) were prepared in 18.2 M $\Omega$  cm Millipore water. Multilayer films were fabricated according to the usual protocol using an automated dipper.<sup>2,8,12</sup> Polished silicon (Si) (100) wafers ( $\sim 100$  mm diameter and  $\sim 6$  mm thick) were purchased from Wafer World Inc. and used as substrates. The wafers were cleaned in concentrated chromium (III) oxide/sulfuric acid for at least 12 h and then thoroughly rinsed with deionized and Millipore water. The solution pH of the polyelectrolytes was adjusted to 3.5 using HCl. The substrates were then alternately immersed into PAH and then PAA baths for 15 min. Between each deposition step, the films were successively immersed into three rinse baths of Millipore water for 1, 2, and 2 min, respectively. The process was repeated until the desired number of layers was deposited (i.e., 18 bilayers). Most experiments reported here were performed with these PAA-capped multilayers. In order to study the effect of the cap layer some experiments were done where an additional PAH layer was added for a total of 18.5 bilayers. In the case of salt-assembled films, 0.2M NaCl solutions were used for the polyelectrolyte solutions and rinse baths. A total of nine bilayers were deposited. After the films were assembled, excess water was removed under a stream of compressed nitrogen. For salt-assembled films, the surface was quickly rinsed with MilliQ water in order to remove any excess salt on the film. The assembled films were then dried under vacuum at 65 °C overnight, and then stored under vacuum until used for measurements.

### Neutron reflectometry and data analysis

Neutron reflectometry experiments were performed at the C5 spectrometer (Chalk River Laboratories, ON). Measurements were performed in specular reflection mode as a function of the momentum transfer  $q_z = (4\pi/\lambda)\sin\theta$ , in the range of 0.006–0.08 Å<sup>-1</sup>, where  $\lambda$  is the fixed incident neutron wavelength of 2.37 Å. The resolution of the measurements was varied in discrete steps by changing collimation at several scattering angles. The count times were adjusted accordingly so that proper count statistics were maintained throughout the entire scan. A constant (full width at half maximum) resolution of  $\Delta q_z/q_z = 0.045$  was maintained. Background scattering was measured off specularly with a fixed angular displacement of the sample of  $-1^\circ$  for the measurements on dry samples and  $-0.15^\circ$  for the samples in the liquid cell. The data were normalized by the incident beam intensity to account for the variations due to the changing slit widths. The samples were placed into an environmental chamber where the temperature and solvent conditions could be controlled.<sup>13</sup> The sample stage was maintained at 25 °C for all experiments and for dry scans the films were kept dry in the cell with a nitrogen purge. Bulk water swelling studies were carried out using 100% D<sub>2</sub>O. The pD of the solutions was adjusted with either NaOD or DCl. To deconvolute the contributions of the swollen PEM matrix and counterions from water uptake within the film, swelling experiments were also conducted using null-scattering water. This solvent

mixture has a net scattering length density of 0, and therefore only the PEM matrix and the counterions contribute to neutron scattering intensity. The water or counterion distribution within the film was then obtained by simply subtracting the SLD profile from the original (100% D<sub>2</sub>O) scattering curve [refer to Eqs. (1) and (2)]. In the case of the experiments with the null-scattering water, the lack of a critical edge required the reflectivity curve to be normalized with the corresponding 100% D<sub>2</sub>O normalization factor. Various salt (NaCl, LiCl, and KCl) solutions were prepared in either D<sub>2</sub>O or null-scattering water. The films were exposed to the salt or pD solutions for a minimum of 7 h. Verification scans were performed which demonstrated that the measured film profiles were stable over the course of the 8–12 h measurement span. The scattering length density profiles of the films were fitted with Parratt's dynamic approach,<sup>14</sup> using the PARRATT32 fitting software (provided by HMI, Berlin, Germany). The instrumental resolution was included when fitting the reflectivity curves. The silicon dioxide thickness and roughness were fitted from neutron reflectivity curves obtained from bare Si wafers of the same batch as those used as substrates for multilayering. A simple one-box or two-box model of the polymer film was insufficient in producing reasonable fits to the data especially for the cases where the samples were swollen or with dry film that had been exposed to salt solutions. A three- or four-box model was used to fit the reflectivity curves, where single thin slabs were used to model polymer/substrate and polymer/environment interfaces. A larger slab was used to model the bulk interior of the multilayer. All parameters (e.g., film/substrate roughness, internal roughness, film/air roughness, and the SLD of the polymer slabs) were free to evolve except for the SLD of the substrate and oxide. In the resulting SLD profiles, we have chosen to define  $z=0$  as the silicon/oxide film interface.

## RESULTS

### The influence of pD on water distribution

To probe the effect of solution acidity and basicity on the water content within the multilayer, PAH/PAA polyelectrolyte films, assembled at pH=3.5 without salt, were exposed to solutions of varying pD (3.0, 6.3, 7.0, and 8.0) in 100% D<sub>2</sub>O (the deuterated solvent provides strong scattering contrast for neutron measurements). Figure 1 shows the neutron reflectometry data taken for films exposed to pD solutions inside the environmental chamber, as well as the corresponding best-fit film profile (for data on the films prior to aqueous exposure, refer to EPAPS data, Fig. 1).<sup>15</sup> The SLD profile throughout the film swollen in pure D<sub>2</sub>O (pD=6.3) is not uniform, indicating that water segregates preferentially to the free surface of the film and does not penetrate efficiently to the substrate interface. This gradient in water affinity is consistent with our previous studies on swollen PEM films,<sup>8</sup> but Fig. 2 demonstrates clearly that this effect can be tuned via solvent conditions. In particular, when the aqueous solvent deviates substantially from neutral, water is able to penetrate uniformly throughout the film.

This trend is better illustrated in Fig. 2 where the film

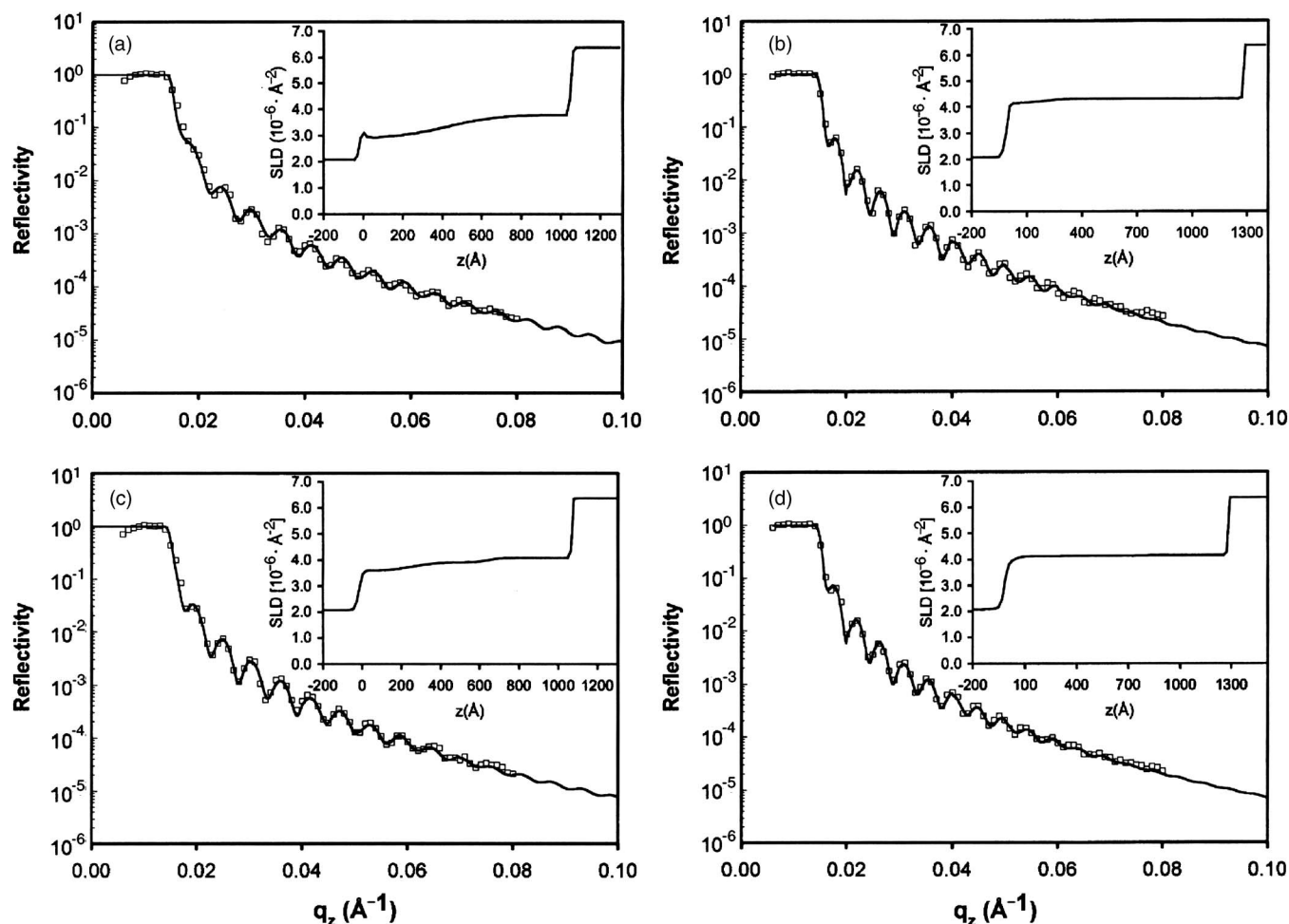


FIG. 1. Neutron reflectometry data in the hydrated state (error bars are within the size of the symbols) and fit (solid continuous lines) for PAA/PAH films assembled at  $pH=3.5$  and exposed to  $D_2O$  at various  $pD$  values: (a) ( $pD=6.3$ ), (b)  $pD=7.0$ , (c)  $pD=8.0$ , and (d)  $pD=3.0$ . The insets to the figures show the resultant SLD profiles. The corresponding reflectivity data and SLD profiles of the dry films are shown in EPAPS, Fig. 1 (Ref. 15). Note: (c) and (d) 1 have the same corresponding dry film profile [EPAPS, Fig. 1(c)].

thickness has been normalized. In addition to the strong asymmetry in the SLD profile for the sample in  $pD=6.3$ , there is also less  $D_2O$  incorporated into this film compared to the others. As the  $pD$  of the solution is increased from  $pD=6.3$ , the SLD profiles become more uniform, as a result of more water being incorporated by the film. Similarly the

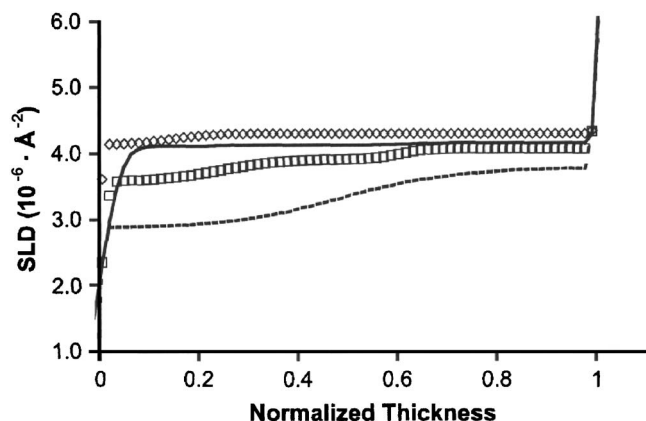


FIG. 2. SLD profiles of films normalized to the same thickness, under solution conditions of  $pD=6.3$  (dashed line),  $pD=7.0$  ( $\square$ ),  $pD=8.0$  (solid line), and  $pD=3.0$  ( $\diamond$ ).

acidic condition ( $pD$  3.0) allows more solvent to swell the film, producing a more uniform SLD profile. This increase in the absorption of  $D_2O$  by films with a  $pD$  value higher or lower than 6.3 can be attributed to the effect of the strong  $pD$  change imposed on the ionizable PAA and PAH groups (films are exposed to  $pH \sim 5.5-6.5$  during the rinsing steps in the assembly process). At higher  $pD$  values, the free carboxylic acid groups on the PAA chains become more charged (to near 100%  $COO^-$  groups at  $pD=8.0$ ),<sup>16</sup> whereas the free amine groups of PAH become less charged. This results in a self-repulsion of the polyelectrolyte chains that enhances the porous structure of the film, which leads to a greater  $D_2O$  content in the film and to greater permeability toward the substrate. Similarly, when the film is exposed to a lower  $pD$  value (3.0), the amine groups of the PAH chains became fully charged, while the charge fraction on the PAA chains decreases, leading to a similar charge inequality. This also may lead to a more diffuse film structure that can facilitate an enhanced permeability of  $D_2O$  toward the substrate. It is also possible that the greater number of ionic groups present in the film after exposure to non-neutral aqueous conditions could alter water uptake by changing the proportion of ionic

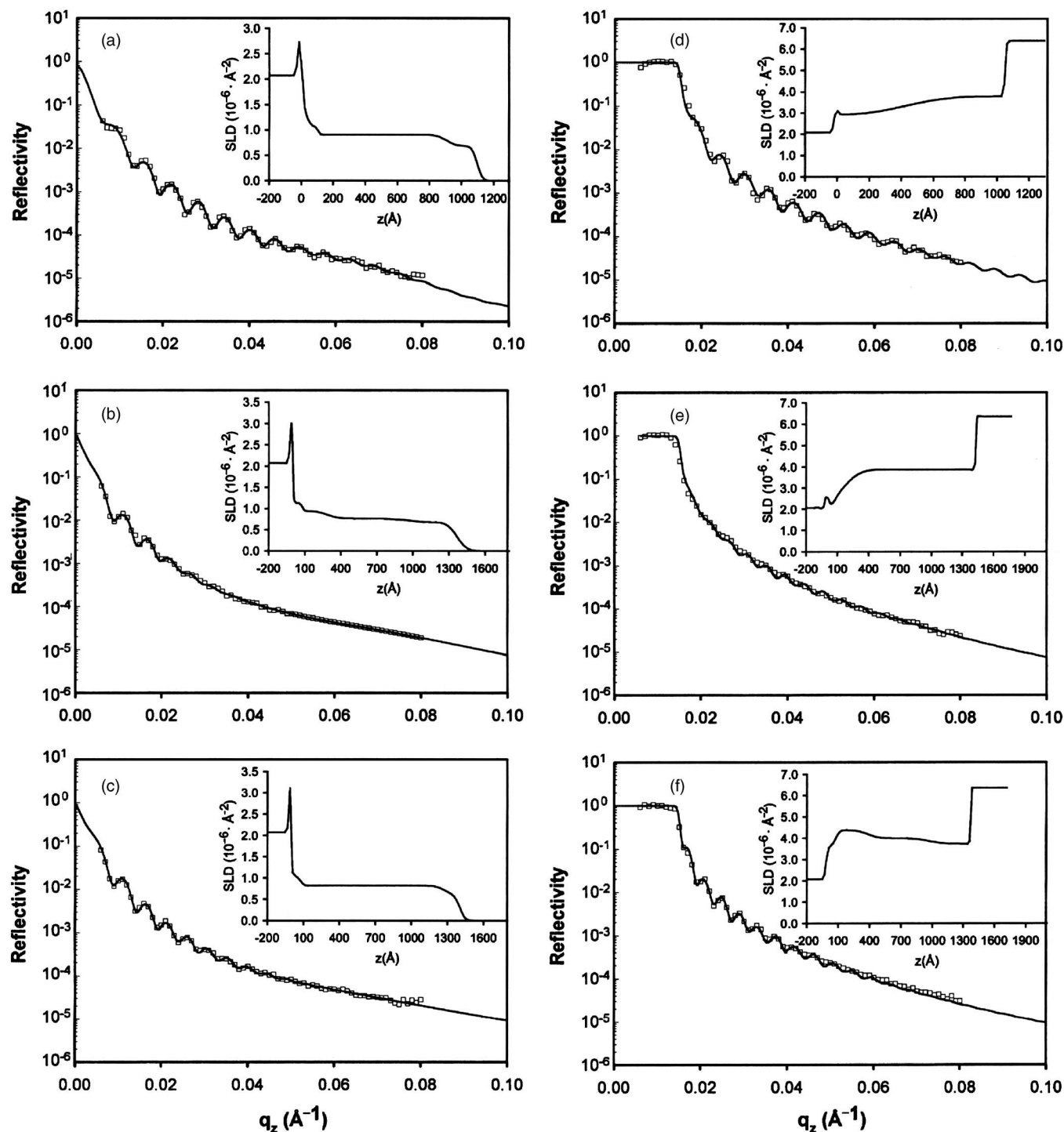


FIG. 3. Neutron reflectometry data (error bars are within the size of the symbols) of films hydrated in null-scattering water [(a)–(c)] and  $D_2O$  [(d)–(f)] solvent. The solid lines are fits to the data, the corresponding SLD profile obtained from fits to the data are shown in the insets to the figures. (a) Exposed to null-scattering water with no salt added, (b) exposed to a solution of 0.1M NaCl, and (c) exposed to a solution of 0.2M NaCl. The corresponding reflectivity data and SLD profiles for the films exposed to  $D_2O$  solutions with an ionic strength of (d) no added salt, (e) 0.1M NaCl, and (f) 0.2M NaCl.

sites for water to cluster. Nevertheless, the films expanded to the same extent regardless of the  $pD$  solution, consistent with previous studies.<sup>9</sup>

### The influence of ionic strength

To determine the effect of the ionic strength on the water distribution within multilayers, we measured films exposed to solutions of varying NaCl concentrations in pure  $D_2O$  and

with null-scattering water. Figure 3 shows the data for three salt concentrations (0.0M, 0.1M, and 0.2M), both, in null-scattering water, where the best-fit profile thus corresponds to the underlying film plus salt, and in pure  $D_2O$ , where the profile corresponds to the sum of film, water, and salt. With increasing salt concentration, the SLD near the substrate interface increases, suggesting that water is now penetrating deeper into the film. The SLD profile of solvent within the

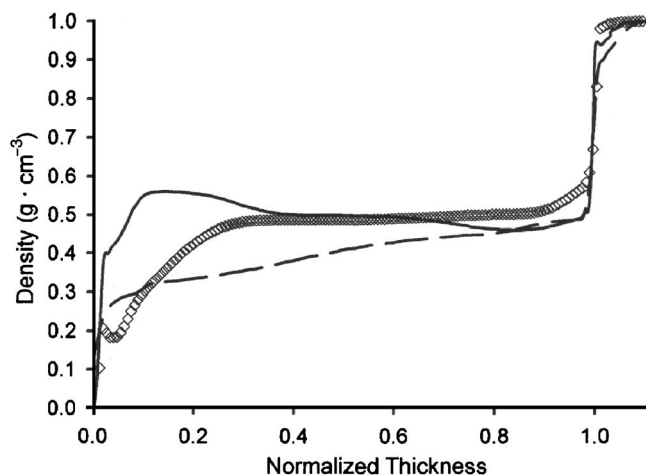


FIG. 4. Water distribution in PAA/PAH multilayer films assembled at  $pH=3.5$  and hydrated using: pure  $D_2O$  (dashed line),  $D_2O$  with  $0.1M$  NaCl (open symbols), and  $0.2M$  NaCl (solid line) added.

film was then deconvoluted by subtracting the contribution of the underlying swollen film (swelling experiments with null-scattering water as shown in Figs. 3(a)–3(c)) from the water-inclusive data [100%  $D_2O$ , Figs. 3(d)–3(f)]. Specifically, the deconvolution was performed using the following equation:

$$d(z) = \frac{SLD_{100\%D_2O}(z) - SLD_{null-scattering}(z)}{b_{D_2O}} m_{H_2O}, \quad (1)$$

where  $d(z)$  is the water density profile in the film normal ( $z$ ) direction,  $SLD_i(z)$  is the best-fit scattering-length density profile for the measurement condition  $i$ ,  $b_{D_2O}$  is the scattering length of pure  $D_2O$ , and  $m_{H_2O}$  is the molar mass of water. Figure 4 shows the resulting profile, which is necessarily only due to water. The water distribution within the multilayer is again strongly nonuniform when the film is exposed to low ionic strength water, and the water appears predominantly localized at the film–ambient interface and does not completely penetrate toward the substrate, in agreement with previous studies.<sup>8</sup> The sharp interface seen in the water profile is also consistent with the previous measurements. The water fraction associated with the outer layer is  $\sim 54\%$ , while in the bulk region of the film the water fraction content ranges from  $\sim 45\%$  to  $35\%$ . When the film was exposed to a solution of  $0.1M$  NaCl, however, the water fraction in the bulk region of the film became more uniform, near  $\sim 50\%$ , while the water fraction associated with the outer layer was  $\sim 60\%$ . There is also a small decrease in water content near the substrate interface, but the overall water content in the film has clearly increased as compared to the salt-free case. When the film was exposed to a  $0.2M$  NaCl solution, the overall water content in the film increased even more substantially, with a substantial  $\sim 56\%$  water density observed near the substrate. The increase in the water content in the film when exposed to salt solutions can be attributed to a screening effect. As the ionic strength of the solution increases, shielding of the charges on the polyelectrolyte chains in the multilayer increases, and a decrease in

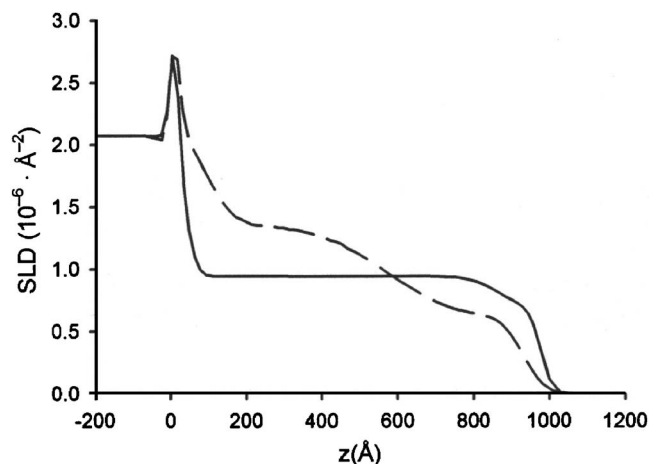


FIG. 5. SLD profiles of PAA/PAH multilayer films assembled at  $pH=3.5$  in the dry state prior to exposure to salt solutions (solid line) and then after exposure to multiple salt solutions:  $0.2M$  LiCl and  $0.2M$  KCl  $100\%$   $D_2O$  solutions (dashed line).

the electrostatic interaction between the chains results. The decrease in the electrostatic interaction between the chains leads to the formation of a more diffuse film structure that enhances the permeation of salt ions (used to extrinsically compensate the free charges) and additional waters of hydration into the film, as observed. The polyelectrolyte segments associated with the salt counterions are more hydrophilic, and therefore more water will be associated with the polymer chains.<sup>17</sup> The considerable excess of water near the substrate suggests that either the film architecture (e.g., chain stoichiometry) is slightly different in this film region or that ions preferentially localize in that film region, leading to a larger effect.

### Ion distribution

The solvent-swelling experiments provide insight into the interaction between water and the polyelectrolyte chains, but cannot directly probe ion–film effects. By comparing the SLD profiles of films before and after exposure to salt solutions, the ion distribution in the film, and hence the ion–film interaction, was determined. We used NaCl, KCl, and LiCl because of the large positive scattering length of  $9.58$  fm for chlorine, which makes it easy to detect with neutron reflectometry. This can be seen in Fig. 5 where a typical film profile before and after exposure to salt solution (refer to EPAPS data, Fig. 2, for the corresponding reflectivity curves).<sup>15</sup> A considerable increase in the SLD near the substrate, and throughout much of the film bulk, is evident. This indicates that salt ions permeate into multilayers during swelling and localize into the film. The final concentration of ions segregated into the film is much higher than in the swelling solution, indicating a strong interaction between the ions and the polyelectrolyte chains in the film. Furthermore, the much higher concentration of ions near the substrate indicates that the film's architecture in this region provides more interaction sites for ion segregation. Using the inferred molecular volume and the known scattering length of KCl, the amount of ions present per repeat unit can be calculated by subtracting the underlying SLD of the dry film prior to

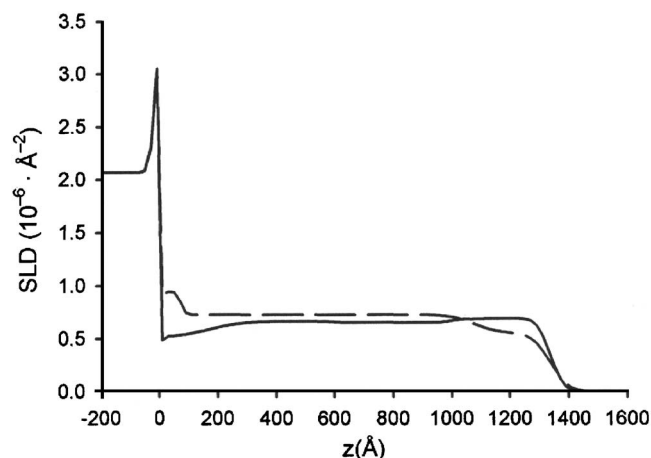


FIG. 6. SLD profiles of a multilayer film in the hydrated state during exposure to a solution of  $0.2M$  LiCl with null-scattering water (solid line) and during exposure to  $0.2M$  KCl with null-scattering water (dashed line).

exposure to the salt solution from the SLD of the film (dry) that was exposed to the salt solution. The numbers of KCl ions per repeat unit (i.e., per single PAH/PAA association group) were calculated to be 0.77 at a distance of  $300 \text{ \AA}$  from the substrate and 1.53 at a distance of  $100 \text{ \AA}$  from the substrate.

The decrease in the SLD profile near the free surface of the film after exposure to the salt solutions could arise from material loss or rearrangement of the polymer chains due to the relatively harsh conditions, high salt conditions that the film was subjected to. It is also possible that the apparent decrease in the dry SLD profile near the surface could be due to the presence of lithium ions that associate with the free  $\text{COO}^-$  groups that are present in the PAA capping layer. Lithium ions have a negative scattering length ( $-1.9 \text{ fm}$ ), whereas potassium has a large positive scattering length ( $3.67 \text{ fm}$ ). It is therefore possible that the potassium ions have not completely exchanged with the lithium ions near the film surface and hence results in the apparent lower SLD profile near the surface. In addition a nonstoichiometric exchange of ions would have to occur, with more lithium ions associated with  $\text{Cl}^-$  in that region. However, incomplete and nonstoichiometric exchange of ions is not likely the case as suggested by experiments with null-scattering water, presented in Fig. 6 (see also EPAPS, Fig. 3).<sup>15</sup> In the case of the experiments with the null-scattering water, only the contribution of the swollen polymer film and the salt ions contribute to the measured reflectivity. Here the SLD profile for the  $0.2M$  KCl is higher in the bulk region due to the positive scattering length of potassium. The overall SLD is lower in the case of  $0.2M$  LiCl since lithium has a negative scattering length. The number of ions per repeat unit (potassium ions that displaced the lithium ions) can be calculated from this using the inferred molecular volume (based on the dry salt-free SLD of the film), the scattering length difference of potassium and lithium ( $5.57 \text{ fm}$ ), and by subtracting the SLD profile of LiCl from KCl. The number of exchangeable cations per repeat unit was determined to be 1.32 at a distance of  $100 \text{ \AA}$ . In the bulk region of the film ( $700 \text{ \AA}$  from the substrate) the number of ions per repeat unit was calculated

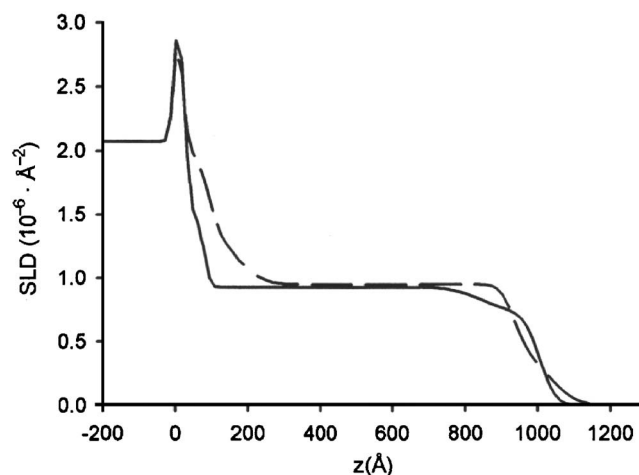


FIG. 7. SLD profiles of a multilayer film, both measured in the dry state; prior to exposure to salt solutions (solid line) and after exposure to  $0.2M$  LiCl with null-scattering water (dashed line).

to be 0.48. However, as seen in the SLD profile for the film exposed to  $0.2M$  LiCl (Fig. 6) with a null-scattering water, the SLD is higher near the free surface, suggesting that small amounts of lithium ions are present at this interface. The decrease in the SLD at the free surface in the dry film (Fig. 5) has not been observed in the other films studied without prior *pD* treatment, implying that the decrease is caused by a loss of material or rearrangement of the polymer chains due to the previous *pD* treatments.

Figure 7 shows additional evidence for salt localization in multilayers. The data show a buildup of salt ions near the substrate after exposure to multiple salt solutions ( $0.2M$  NaCl, followed by  $0.2M$  LiCl, in null-scattering water). Assuming that the LiCl completely displaces the NaCl, and that the chains are 100% hydrogenated, the amount of LiCl ions per repeat unit of  $100 \text{ \AA}$  from the substrate was determined to be 1.81, whereas a much lower amount (0.08) of salt ions is found in the bulk region. The ion content in the films is much higher than the concentration in the bulk solution. That is, the salt ions preferentially migrate into the films and do not merely diffuse into the multilayer. The effect of the cation type on the film's water distribution was also investigated. Figure 8 shows the deconvoluted water profile inside films swollen with  $0.1M$  LiCl and NaCl (see EPAPS, Fig. 5).<sup>15</sup> The resulting profiles suggest that the water distribution in the film is similar, within experimental uncertainty, regardless of salt type ( $0.1M$  salt).

### The effect of the capping layer

The extent of diffusion of salt ions into and out of a PAA/PAH multilayer film was studied as a function of the identity of the polymer at the free surface (the capping layer). In principle changing the capping layer alters the electrostatic charge that the multilayer film presents to solution, which can affect ion diffusion and uptake. Furthermore, by comparing films with salt inclusion after exposure to pure water, we estimate the extent of ion release. Figure 9 shows film profiles for a PAH-capped multilayer (see raw data in EPAPS, Fig. 6).<sup>15</sup> Exposure to a  $0.1M$  LiCl solution resulted

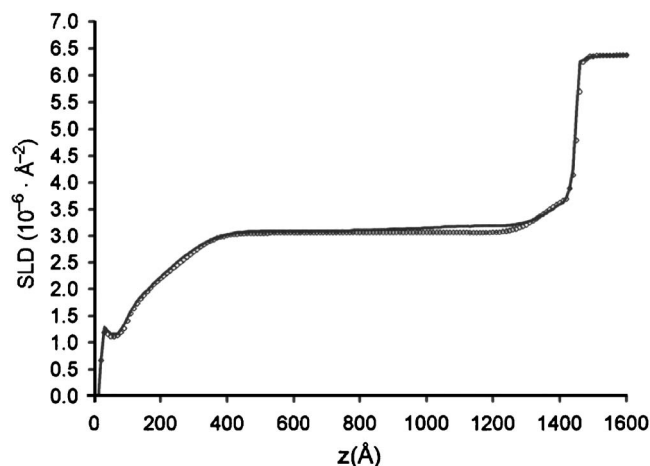


FIG. 8. Differences in water distribution profiles between multilayer films exposed to 0.1M NaCl and 0.1M LiCl solutions. The solid line corresponds to the water distribution in the film when exposed to a solution of 0.1M NaCl, while the open symbols correspond to a solution of 0.1M LiCl.

in an overall increase in the SLD profile with a large increase in the SLD near the substrate. Thus the PAH-capped film exhibits ion localization to the substrate, consistent with the PAA-capped films. The distribution of the LiCl ions throughout film thickness was calculated, and is presented in Fig. 10 (solid line), using the following equation:

$$n(z) = \frac{SLD_{\text{after-exposure}}(z) - SLD_{\text{before-exposure}}(z)}{b_{\text{LiCl}}}, \quad (2)$$

where  $n(z)$  is the number-density profile for ions (assumed to all be LiCl in this case),  $SLD_i(z)$  is the best-fit scattering-length density profile (where “before” refers to the film prior to exposure to any solution and “after” refers to postexposure condition described in Fig. 10; all measurements were performed on dry films), and  $b_{\text{LiCl}}$  is the scattering length of LiCl. The number of salt ions per unit volume was thus estimated using the difference between the dry SLD profile

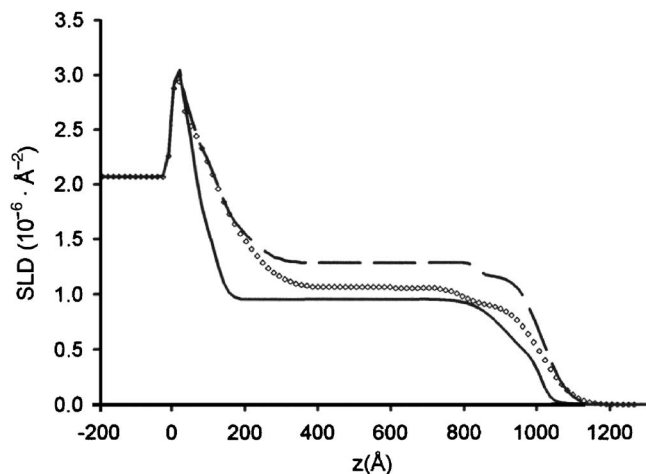


FIG. 9. SLD profile for a dry, PAH capped multilayer film. The solid line is the SLD profile of the film prior to exposure to a salt solution. The dashed line is the SLD profile of the film that was dried after exposure to a 0.1M LiCl solution and the open symbols is the dry SLD profile of the film after it was exposed to H<sub>2</sub>O. Salt ions accumulate in the film and segregate preferentially near the substrate. Rinsing removes some ions but does not displace the ions near the substrate interface.

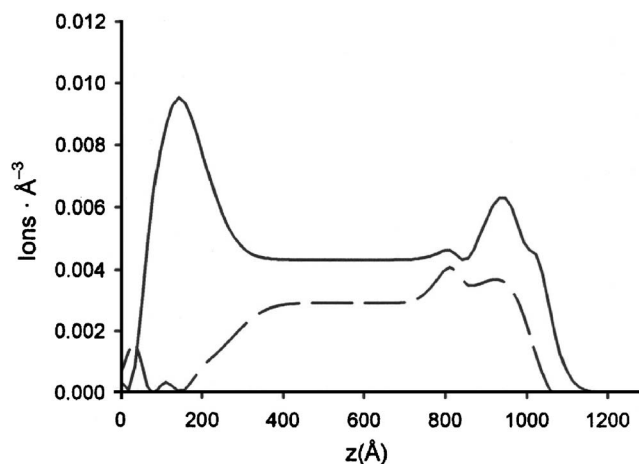
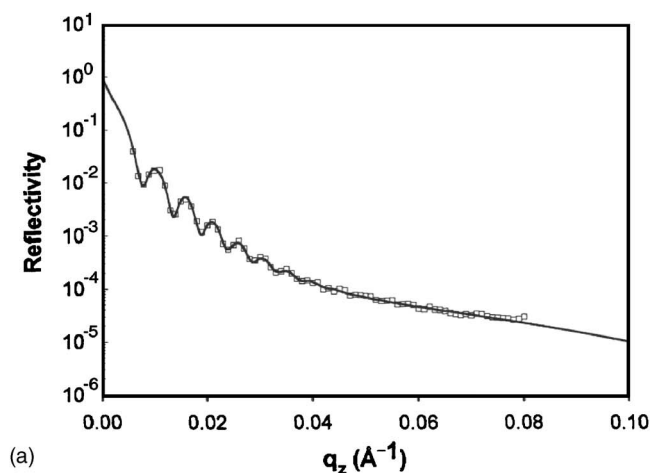


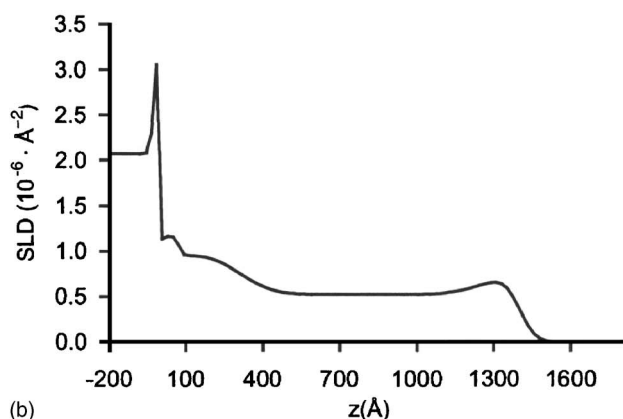
FIG. 10. Ion distribution in a dry, PAH capped multilayer film. The solid line represents the LiCl ion distribution in a multilayer film after exposure to 0.1M LiCl solution. The diffusion of LiCl ions from the film after exposure to MilliQ water is represented by the dashed line.

after exposure to a 0.1M LiCl solution and the underlying SLD profile for a dry film before exposure to a salt solution. As previously stated, there is a higher concentration of salt ions near the substrate, as well as a pronounced increase in the SLD near the free surface of the film. As will be discussed later, the increase in the SLD near the free surface of the film may be due to a capping layer effect. The number of ions per repeat unit was calculated to be 2.0 at a distance of 100 Å from the substrate. This amount was determined in the usual manner described previously (i.e., by subtracting the original underlying dry SLD profile from the dry LiCl profile, using the inferred molecular volume from the dry profile and the scattering length of LiCl). In the bulk region of the film (700 Å from the substrate) the number of ions per repeat unit was determined to be 1.13. After exposure to water the SLD profile decreased, which suggests that LiCl ions diffused out of the film into solution. However, the extent of the salt ion diffusion out of the film was not 100%, as indicated by the slightly higher SLD in the bulk region of the film relative to the original dry film SLD. In addition, the diffusion of the salt ions out of the film did not affect the SLD near the substrate and suggests the strong affinity of the salt ions for the polymer chains in this region. The diffusion of LiCl ions from the film is shown in Fig. 10 (dashed line) as inferred by the difference between the SLD profiles of the dry film after exposure to a 0.1M LiCl solution and water. This clearly indicates that the diffusion of the salt ions occurs primarily in the bulk and outer region of the PEM film. The number of ions that have diffused out of the film in the bulk region (700 Å from the substrate) was determined to be 0.77 per segment, which corresponds to a depletion of ~68%.

The effect of the capping layer is evident in Fig. 11. The resulting SLD profile when exposed to null-scattering water, where only the polymer and salt ions contribute to the reflectivity data, reveals the usual increase in the SLD near the substrate. However, there is also an increase in the SLD near the free surface of the film, which is also apparent in the dry profile after salt exposure (Figs. 9 and 10). It is possible that this increase in the SLD near the free surface is due to the



(a)



(b)

FIG. 11. (a) Neutron reflectometry data of a PAH capped multilayer film hydrated in null-scattering water containing 0.1M LiCl (error bars are within the size of the symbols). The solid line is the fit to the data. (b) The corresponding SLD profile.

association of  $\text{Cl}^-$  ions with the free amine groups of the PAH layer capping layer. Chlorine has a very large scattering length (9.58 fm), in comparison to lithium (-1.9 fm) and sodium (3.63 fm), and can be easily differentiated at the surface of the film.

Calculating an inferred swollen SLD from a dry film (prior to salt solution exposure) gives values in the bulk region that are much higher ( $6.7 \times 10^{-7} \text{ \AA}^{-2}$ ) than those obtained experimentally when exposed to salt solutions (Fig. 11,  $\text{SLD} = 5.2 \times 10^{-7} \text{ \AA}^{-2}$ ). For this to be possible there would have to be more  $\text{Li}^+$  incorporated into the bulk of the multilayer. The SLD value in the bulk region of the film is lower than for the films assembled without a PAH capping layer. It is therefore more likely that there is a nonstoichiometric diffusion that occurs. Under the assembly conditions, PAH is fully charged and PAA is partially charged ( $\sim 75\%$ ). It is therefore possible that as the salt ions diffuse into the film, more lithium ions will associate with the free carboxylic acid groups in the film. This would lead to the apparent decrease in the SLD in the bulk region of the film.

### Ion distribution in salt-assembled films

The distribution of ions in films assembled in the presence of salt was also investigated. Figure 12 shows the best-

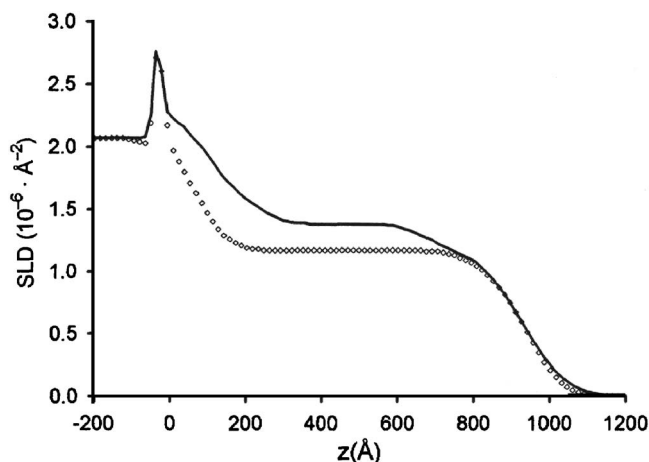


FIG. 12. SLD profile for a dry assembly  $\text{pH}=3.5$  PAA/PAH multilayer film assembled with 0.2M NaCl. The solid line is the SLD profile of the film prior to exposure to a salt solution. The open symbol is the SLD profile of the film that was dried after exposure to a 0.2M NaCl and 0.2M LiCl solution.

fit SLD profiles for an assembly  $\text{pH}=3.5$  PAA/PAH multilayer film assembled with 0.2M NaCl before and after exposure to a solution of 0.2M LiCl in pure  $\text{D}_2\text{O}$ . The overall SLD of the dry film assembled with 0.2M NaCl is greater than those that were not assembled in the presence of salt. This increase in the SLD is due to the high scattering length of  $\text{Cl}^-$  (9.58 fm) and  $\text{Na}^+$  (3.63 fm) ions that extrinsically compensate the multilayer film. Furthermore, the region near the substrate of the film has a higher SLD than the bulk region and suggests that salt ions preferentially localize near the substrate of the film. This behavior is identical to salt-free films exposed to salt after assembly. Thus, the localization of ions to the substrate interface appears to be an effect intrinsically connected to the film architecture in that region, rather than due to a “diffusion barrier” produced by the film’s external layers. After exposure to a solution of 0.2M LiCl in pure  $\text{D}_2\text{O}$ , the SLD of the dry film decreased in the bulk and near the substrate regions of the film. This suggests that the sodium ions that were originally incorporated into the multilayer have been displaced by the lithium ions. The amounts of  $\text{Na}^+$  displaced by  $\text{Li}^+$  ions per repeat unit were determined to be 1.02 in the bulk region of the film (500 Å from the substrate) and 2.28 near the substrate (100 Å from the substrate).

### DISCUSSION

The methodology presented in this paper exploits the variable scattering length densities of the solvents and ions used, making it possible to accurately determine the localization of species within thin films. In particular, the ability to mix  $\text{H}_2\text{O}$  and  $\text{D}_2\text{O}$  in order to generate a null-scattering water enables us to extract the water distribution profile across thin films. Moreover, the differing scattering lengths possessed by the salt ions enable us to determine whether the incorporated ions are displaced after subsequent solvent treatments. Although fitting the data is somewhat challenging, the data presented here contain a number of recurring features that enable us to arrive at plausible conclusions. In

particular, it is evident that thin polyelectrolyte films incorporate salt ions efficiently. In fact, the concentration of ions in the film is greater than in the bulk solution, indicating that ion affinity, and not merely ion diffusion, is responsible for the uptake. Moreover, all of the SLDs presented indicate that salt concentrates in the vicinity of the film/substrate interface. This effect occurs regardless of whether the film is exposed to salt solutions after the assembly process or during the assembly, indicating that it is intrinsic to the film's structure, and not due to a diffusion barrier generated by the film layers. Consistent with previous investigations, this suggests that the first few layers of multilayer buildup differ (e.g., in architecture and polyelectrolyte chain stoichiometry) from the film bulk. This is reasonable considering that this interface region presents a charge density unequal to the film's interior.

The measurably different film properties near the substrate lead to salt localization, affecting the distribution of water throughout the film. Whereas in the absence of salt, water is unable to penetrate to the film/substrate interface, addition of salt modifies the film's structure (probably screening charges and generating a more porous network), allowing access to water. In fact, sufficiently high salt concentrations led to water preferentially occupying this salt-rich region. A qualitatively similar behavior is seen by adjusting the solution  $pH$  (or  $pD$ ). In this case, the change in solution  $pH$  affects the degree of ionization of the polyelectrolyte repeat units. At strongly non-neutral  $pH$  values (either acidic or basic), the imbalance in chain charge leads to statistically fewer sticker groups, generating a more porous network amenable to water penetrating uniformly throughout the film. Importantly, it should be noted that while  $pH$  adjustment could alter water localization, allowing for the uniform distribution throughout the film structure,  $pH$  treatment alone did not result in water accumulating at the film/substrate interface. Thus, the observed water buildup near the substrate observed with salt swelling is intrinsically related to the presence of the salt, which not only alters the structure (e.g., porosity) of the film matrix but also draws in additional water.

With respect to the ion association with the polyelectrolyte film, the present experiments strongly indicate that the association is pseudothermodynamic and not a purely kinetic effect. This is supported by the fact that some of the ions migrate out of the film upon exposure to water solutions, and moreover by the experiments wherein one type of salt ion was exchanged for another. Nevertheless, the fact that salt-laden films exposed to pure water conditions retained much of their salt indicates a strong interaction between the ions and the polyelectrolyte matrix. This interaction is evidently not uniform throughout the film: the ions near the surface were more readily lost, whereas the ions associated with the near-substrate region were not lost during pure water treatment. This indicates that there is a strong preferential association of ions with this part of the film. Thus the strong ion affinity for the film/substrate interface is supported both by the accumulation of ions in that region, and the presence of these ions even after rinsing.

Careful analysis of the SLD values has indicated that the

ion diffusion into the film is more likely not strictly stoichiometric, which is consistent with the assumption that these ions are inherently entering the film in order to compensate for the charges on free polyelectrolyte groups. During assembly, the PAA and PAH chains are not identically charged, and thus will require different levels of charge compensation. The quantity of ions accumulated in the film was also calculated (based on known SLD values), and it was found that ion association is of the order of being near stoichiometric with the repeat units. That is, the included salt ions are associating with the polyelectrolyte chains. This inclusion of salt not only occurs due to local architecture (chain stoichiometry and chain charge) but also alters the film architecture by screening the interaction between chains. Thus there may also be autocatalytic effects of solvent/ion inclusion, some evidence of which were seen in swelling kinetic experiments.

## CONCLUSIONS

Neutron reflectometry experiments have provided a means to examine the water and counterion distribution in weak PEM films. It is evident that exposing the films to a  $pH$  above or below that of the rinse bath results in an enhancement of water permeation. An increase in water penetration into the films was also observed in films exposed to various salt solutions, with water content increasing with increasing local salt concentration. The present results clearly demonstrated the strong affinity that salt ions have for polyelectrolyte films. In particular, salt ions preferentially localized near the substrate of multilayer/substrate interface, where the film's architecture more likely deviates from the bulk. This effect was observed both in the case of film exposure to salt solutions after assembly or during assembly, suggesting that it is intrinsic to the film's organization. Finally, although the capping layer strongly influenced the ion distribution in the film, an enhanced ion content near the substrate was still observed.

## ACKNOWLEDGMENTS

The authors would like to thank the Canadian Neutron Beam Centre, NRC Chalk River Laboratories for beam time. Funding was provided by the McGill FQRNT Centre for Self-Assembled Chemical Structures and NSERC Canada.

<sup>1</sup>G. Decher, *Science* **277**, 1232 (1997).

<sup>2</sup>S. S. Shiratori and M. F. Rubner, *Macromolecules* **33**, 4213 (2000).

<sup>3</sup>S.-H. Lee, J. Kumar, and S. K. Tripathy, *Langmuir* **16**, 10482 (2000); J. Dai, A. W. Jensen, D. K. Mohanty, J. Erndt, and M. L. Bruening, *ibid.* **17**, 931 (2001).

<sup>4</sup>L. Zhai, A. J. Nolte, R. E. Cohen, and M. F. Rubner, *Macromolecules* **37**, 6113 (2004).

<sup>5</sup>A. J. Nolte, M. F. Rubner, and R. E. Cohen, *Langmuir* **20**, 3304 (2004).

<sup>6</sup>J. Dai, A. M. Balachandra, J. I. Lee, and M. L. Bruening, *Macromolecules* **35**, 3164 (2002); W. Jin, A. Toutianoush, and B. Tieke, *Langmuir* **19**, 2550 (2003); M. D. Miller and M. L. Bruening, *ibid.* **20**, 11545 (2004).

<sup>7</sup>X. Shi and F. Caruso, *Langmuir* **17**, 2036 (2001); G. B. Sukhorukov, A. A. Antipov, A. Voigt, E. Donath, and H. Möhwald, *Macromol. Rapid Commun.* **22**, 44 (2001); A. J. Chung and M. F. Rubner, *Langmuir* **18**, 1176 (2002); C. M. Nolan, M. J. Serpe, and L. A. Lyon, *Biomacromolecules* **5**, 1940 (2004).

<sup>8</sup>O. M. Tanchak, K. G. Yager, H. Fritzsche, T. Harroun, J. Katsaras, and C. J. Barrett, *Langmuir* **22**, 5137 (2006).

- <sup>9</sup>O. M. Tanchak and C. J. Barrett, *Chem. Mater.* **16**, 2734 (2004).
- <sup>10</sup>J. Schmitt, T. Gruenewald, G. Decher, P. S. Pershan, K. Kjaer, and M. Loesche, *Macromolecules* **26**, 7058 (1993); A. Fery, B. Schoeler, T. Cassagneau, and F. Caruso, *Langmuir* **17**, 3779 (2001); D. Laurent and J. B. Schlenoff, *ibid.* **13**, 1552 (1997); H. Riegler and F. Essler, *Langmuir* **18**, 6694 (2002).
- <sup>11</sup>V. M. Prabhu, B. D. Vogt, W. Wu, J. F. Douglas, E. K. Lin, S. K. Satija, D. L. Goldfarb, and H. Ito, *Langmuir* **21**, 6647 (2005).
- <sup>12</sup>D. Yoo, S. S. Shiratori, and M. F. Rubner, *Macromolecules* **31**, 4309 (1998).
- <sup>13</sup>T. A. Harroun, H. Fritzsche, M. J. Watson, K. G. Yager, O. M. Tanchak, C. J. Barrett, and J. Katsaras, *Rev. Sci. Instrum.* **76**, 065101/1 (2005).
- <sup>14</sup>L. G. Parratt, *Phys. Rev.* **95**, 359 (1954).
- <sup>15</sup>See EPAPS Document No. E-JCPSA6-129-614825 for supplementary neutron reflectivity data and fits. For more information on EPAPS, see <http://www.aip.org/pubservs/epaps.html>.
- <sup>16</sup>S. E. Burke and C. J. Barrett, *Langmuir* **19**, 3297 (2003).
- <sup>17</sup>S. T. Dubas and J. B. Schlenoff, *Langmuir* **17**, 7725 (2001).